OBSERVATIONS OF NIGHTSIDE AND DAYSIDE AURORAL KILOMETRIC RADIATION WITH VIKING

H. de Feraudy[1], A. Bahnsen[2], and M. Jespersen[2]

[1]*Centre de Recherches en Physique de l'Environment Terrestre et Planetaire, CNET/CRPE, 92131 Issy–les–Moulineaux, France*

[2]*Danish Space Research Institute, 28000 Lyngby, Denmark*

Abstract

A short review of the AKR observations, before the Viking satellite was launched, is presented. The V4H high frequency experiment is briefly described. The Viking observations showed evidence of R–X and L–O mode AKR. The R–X mode waves are confined inside a cone. It is shown that inside the cone, the AKR emissions look like the superposition of discrete narrowband elements. Several examples of AKR source region crossings are presented. The main AKR peak was sometimes observed at – or even below – the electron gyrofrequency, this feature was retained as the signature of the crossing of source regions. The AKR sources appeared as narrow structures, typically 10 to 100 km width, in which the fluxes of low energy electrons had dropped. The examination of particle spectrograms suggested that hot electrons in the source presented ringlike velocity distributions with a loss cone and eventually a lower energy core. An example of strong refraction of the waves at the edges of a source structure is presented. A tight correlation between the location of the ionospheric footprint of the magnetic field–lines passing through AKR sources and discrete auroral arcs is shown. Examples of short duration bursts of AKR observed on the dayside are presented.

1. Introduction

The terrestrial Auroral Kilometric Radiation, AKR, has been observed for the first time by Benediktov et al. (1965). Since then knowledge on its characteristics has accumulated from several experiments.

AKR is a powerful electromagnetic emission; it was estimated that 10^7 to 10^9 Watts are radiated during an event (Gurnett, 1974). Several per cent of the free energy contained in the velocity distribution function of the electrons can be converted into wave energy (Wu et al., 1981a; Wu, 1985; see also for a discussion on convective effects Zarka et al., 1986). Interferometric measurements from the ISEE–1 and –2 satellites showed that these emissions present a high degree of coherency (Baumback et al., 1986) suggesting that AKR sources work as oscillators rather than amplifiers of a background electromagnetic noise. The frequency range of AKR is 50 – 700 kHz with, on the average, a peak intensity around 200 kHz. AKR events present two kinds of substructure. At first, a high frequency resolution analysis reveals a complex structure of narrow band elements with a time drifting center frequency (Gurnett et al., 1979a). Assuming that the waves are emitted close to the electron gyrofrequency, Gurnett and Anderson (1981) proposed that this could be caused by potential structures drifting along the auroral field–lines with velocities comparable to the ion acoustic velocity. Morioka et al. (1981) showed that these drifting source

structures are decelerated as they move towards the earth. The processing of the analog telemetry data of the ISEE–1 satellite allowed Baumback and Calvert (1987) to show that the instantaneous bandwidth of the AKR components can sometimes be narrower than 10 Hz. The authors concluded that this substantiates a lasing mechanism inside a narrow plasma structure, as was proposed by Calvert (1982). A second kind of substructure of AKR is an harmonic generation at multiples of the electron gyrofrequency f_{ce} (Benson and Calvert, 1979; Mellot et al., 1986 ... and others). The harmonic structure was first attributed to instrumental nonlinear effects, close to the saturation level of the receivers, but presently more and more observations suggest a natural generation. Several wave modes are observed during an AKR event, the predominant waves being extraordinary R–X polarized waves (Kaiser et al., 1978). L–O mode waves are also generated with an average power flux two orders of magnitude smaller than R–X AKR (Mellot et al., 1984). Z mode AKR was also observed; Oya and Morioka (1983) suggested the possibility for AKR to originate from strong Z mode electrostatic emission with subsequent gradual linear conversion to L–O mode through the plasma inhomogeneities. Statistical studies on the spatial extension of the AKR observations showed an angular distribution of the waves nearly isotropic inside a cone, the aperture of which increases with the frequency, from 1.5 π sr at 178 kHz to 0.9 π sr at 56.2 kHz (Green et al., 1977). These authors suggested that the cone was filled. Yet this question is still debated since AKR events presently turn out to consist rather of a superposition of discrete structures than in a wave continuum.

Several characteristics of AKR sources were established, or merely suggested, both from remote observations and in–situ measurements. Evidence for AKR generation over the night side of the auroral oval was first presented by Gurnett (1974) (see also Kurth et al., 1975). This feature was confirmed by Alexander and Kaiser (1976) who used the observations by the RAE–2 lunar orbiter of AKR occultations by the moon. These authors showed evidence for a large dispersion of the AKR source altitudes. Making use of the same instrument, Alexander and Kaiser (1977) suggested the possibility for an AKR generation over the cusps. Yet, Alexander et al. (1979a), discussing this cusp generation, showed that, in fact, these observations could have resulted from the scattering by magnetospheric plasma irregularities of waves generated elsewhere. The average location of the source regions, from the Hawkeye and IMP–6 satellite observations, was found at a geocentric distance of 2.5 earth radii above the night auroral oval, at 70° invariant latitude and 23.00 magnetic local time (Gallagher and Gurnett, 1979). The AKR sources were found to be located inside low density structures where the plasma frequency f_{pe} was smaller than f_{ce}, with, possibly, fine substructures consisting in sharp narrow density enhancements (Benson and Calvert, 1979). Calvert (1981b) showed that the plasma depleted structures formed plasma cavities, several degrees of invariant latitude in width; these cavities, which could extend down to 2000 km in altitude, were broadly field–aligned. According to Benson and Calvert (1979), AKR source region locations coincide with electron inverted V events. These authors suggested the existence of a threshold energy greater than 1 keV for the electrons, below which AKR was not generated. Benson and Akasofu (1984) compared all sky camera pictures and ISIS–1 AKR source crossing observations and showed a strong association between AKR source regions and bright auroral arcs. A weak correlation between intensities of AKR waves and auroral field–aligned current

sheets was found by Saflekos et al. (1982); however it must be remarked that this does not exclude a stronger correlation between the source locations and field–aligned currents of smaller scale.

It is presently admitted that AKR is generated at frequencies close to the fundamental and the harmonics of f_{ce}. The necessity of a low plasma density with $f_{pe} \ll f_{ce}$ for AKR generation can be stated differently, namely $\lambda_{De} \gg \rho_{ce}$, where λ_{De} and ρ_{ce} are respectively the Debye length and the average Larmor radius of the electrons. This simply means that gyromagnetic effects such as phase bunching of the electrons in the velocity space are predominating over space charge screening effects. Several theories were proposed for AKR generation. Grabbe (1981) summarized most of them. It is beyond the scope of this paper to discuss these theories. The salient features, to our feeling, on this subject can be roughly schematized as follows: the Maser Cyclotron Instability (see, for example, Wu, 1985) is the most elaborated theory. It can account for many AKR features, mainly the R–X and L–O mode generation with acceptable relative growth rates, the possibility for harmonic generation, the emission along a cone with an aperture corresponding to the observations. However, the inhomogeneity of the plasma characteristics as well as the one of the geomagnetic field smears out the resonance condition matching over a rather short range of altitudes, which reduces the efficiency of the generation mechanism (Le Quéau et al., 1985; Zarka et al., 1986). A key factor for the efficiency of this mechanism is the density ratio of the suprathermal over the lower energy thermal populations, related to the average energy of the suprathermal electrons. Theories involving linear mode conversion processes from electrostatic Z mode to electromagnetic free escaping modes (e.g. Oya and Morioka, 1983) cannot yet be ruled out. Non linear theories such as those involving whistler solitons interacting with upper–hybrid waves (Buti and Lakhina, 1985) are not as well elaborated, this makes them difficult to be tested with experimental observations. Calvert (1982) proposed a feedback model in which the generated AKR waves are trapped inside narrow field aligned source density structures. If phase tuning conditions are met, the active medium should act as an oscillator (lasing). This mechanism is consistent with the extreme narrow bandwidth of the AKR elements (Baumback and Calvert, 1987).

This short review has no pretention to be exhaustive, its aim is merely to give the reader the means to find his way through the literature.

The Viking high frequency wave experiment is presented in Section 2. Section 3 is dedicated to the Viking observations of AKR. The main features of the AKR wave morphology are presented through an example of AKR event, then we describe AKR source crossings, and we show the tight magnetic conjugacy of auroral arcs and AKR source location. We show that they are not confined to premidnight auroral invariant latitudes. Finally, dayside observations of AKR are shortly discussed.

2. The V4H high frequency wave experiment

The Viking project was managed by the Swedish Space Corporation (SSC). A brief description is given in Hultqvist (1987). The Viking satellite was spin stabilized in a cartwheel mode with a spin rate of 3 r.p.m.. The spinning plane was close to the local magnetic meridian plane so that the radial antennae used by the wave experiment were alternatively perpendicular and nearly parallel to the geomagnetic field direction.

The V4H high frequency wave experiment of the satellite measured one electric component of the waves in the spin plane and one magnetic component parallel to the spin axis, in the frequency range 4 – 700 kHz. At these frequencies the dynamics of the ions can be neglected in the plasma and geomagnetic field environment of Viking. The instrument is described in details in Bahnsen et al. (1985).

The electric field sensors were two spheres mounted at the tips of two opposite 40 m radial wire antennae. These sensors were shared with DC electric field measurements (V1) and the low frequency wave (V4L) experiments. Since the antennae were rotating in a plane close to magnetic meridian planes, the received signals were affected with a modulation at half the spin period when the received waves were well polarized. This enables us to distinguish between waves coming from different places or between waves with different polarizations. The magnetic sensor was an air core loop viewing towards the spin axis. Two kinds of processors were used:

- Batteries of 8 filters for both, electric and magnetic wave components. The center frequencies of these filters were logarithmically spaced in the range 10 – 512 kHz. One spectrum of each component was obtained every 40 ms.

- Two stepped frequency analyzers (SFA), one for each measured wave component. The 10 – 500 kHz frequency range was swept in 256 steps. The frequency resolution was 1, 2 or 4 kHz respectively in the 10 – 128 kHz, 128 – 256 kHz, 256 – 500 kHz frequency ranges. For most of the observations one frequency sweeping throughout 10 – 500 kHz was achieved in 2.4 s, therefore more than 4 spectra were obtained during half a spin period. This produced the deep spin modulation in the intensity of the wave dynamic spectra, which was often observed.

The sensitivity of the instruments was $5{\cdot}10^{-8}$ V/m/$\sqrt{Hz}$ for the electric component and 10^{-1} Teslas/$\sqrt{Hz}$ for the magnetic component.

Fig. 1 (color plot): Dynamic spectra of the high frequency wave observations of orbit 185. The upper part presents 2 hours of observations, the lower part presents the evening AKR event of the same orbit. Each part is made of two spectrograms: the upper one represents the wave magnetic component, the lower one the electric component. The time is marked in white above the electric component spectrogram in the upper part of the figure, and at the top of the lower part. The horizontal green lines are interference lines.

Two active experiments were included in V4H:

1. A relaxation sounder which provided one with an electron density measurement every 2 minutes in standard operations mode, one measurement every 4.8 s in a diagnostic mode.

2. A mutual impedance sounder which also measured the electron plasma temperature when the distribution function of the electron velocities could be modelled as a sum of Maxwellian functions.

3. Viking observations

A first general presentation of the Viking wave observations is given in Bahnsen et al. (1987). We shall present here in more details AKR observations with an emphasis on source crossing and on source region structures and locations.

3.1 Wave morphology of AKR

A spectrogram of the observations along orbit 185 is presented on Figure 1. The lower part of each panel shows the electric wave field data, the upper one the magnetic wave component. The horizontal time axis of the upper panel corresponds to 2 hours of data taking. The vertical frequency axis spans the frequency range 10 – 500 kHz. The telemetry counts corresponding to the spectral amplitude of the wave fields are coded in color, giving a rough measure of the wave field amplitude in dB.

The frequency–time space is separated into two parts by the electron gyrofrequency line (white dots). At about 12.00 UT, the satellite was over the nightside of the auroral oval, at 72.5° invariant latitude, 18.50 MLT (Magnetic Local Time).

Below the gyrofrequency line, VLF waves are observed from the dusk– to the dayside oval at 13.10 UT, when the satellite was located at 9.50 MLT, and 75.6° invariant latitude; the altitude was 13500 km, close the apogee of the satellite. The intensity of the emission faded gradually as the altitude increased. These emissions were mainly whistler mode waves, with sporadic electrostatic bursts.

The AKR is observed above the gyrofrequency line. It was observed over two distinct regions where it presented quite different a morphology. The most intense and structured AKR was received between 11.50 and 12.30 UT when the satellite was over the dusk side of the oval, at altitudes ranging between 6500 and 11500 km. The emissions were clearly electromagnetic, as can be seen from the comparison of the electric and magnetic spectrograms; they presented the characteristic global shape of waves emitted inside a cone. This cone was apparently filled in and this point will be shortly discussed below. The frequency of the observations ranged from the gyrofrequency to about 450 kHz, at 11.58 UT when the altitude was 7900 km. AKR was also observed between 13.25 UT and 13.38 UT. At that time, the satellite was in the dayside at Magnetic Local Time between 9.00 and 9.05, well after Viking had crossed the dayside oval. Dayside AKR observations

commonly presented similar bursty patterns with a few minutes burst duration and a comparable recurrence time as in Figure 1.

The lower panel of Figure 1 presents the dusk part of the same event in an expanded time scale. The emission consists of two parts: an intense core with characteristic bowl shape surrounded by more diffuse and less intense waves. The lower cutoff of the whole AKR emission reached the gyrofrequency line at 11.58 UT. Before this time, the cutoff stayed close to/and above the gyrofrequency line and after 18.58 UT it increased very slowly with time.

The core of the emission consisted presumably of R–X emissions. The more significant criterium for this deduction is the phase of the spin modulation pattern, compared to the orientation of the receiving antenna with respect to the direction of the geomagnetic field (de Feraudy et al., 1987). The fine structure is clearly visible. Most of the elements have a positive slope in frequency – time space, however, an element with apparently infinite slope in frequency–time space is observed at 12.11 UT, above 320 kHz, it cannot be understood if the frequency drift is only attributed to a motion of the AKR source region along a field–line. This suggests the possibility of the observed frequency evolution of the AKR elements to result also from a spatial distribution of the source. The richness of the structures inside the cone of the core emission indicates that the apparently continuous emission is likely to be a superposition of discrete structures which are not always resolved by the instruments; this would mean that in fact the emission cone is empty. The time when the emission was observed at or below the gyrofrequency line was interpreted as a crossing of the AKR source; this will be discussed in further detail in the next section.

Figure 2 shows another AKR event. It presents an electric field dynamic spectrum of 4 minutes of V4H observations. In this figure, the high frequency part of the scale is compressed towards the higher frequency. The red line indicates the electron gyrofrequency.

The spin modulation of the signal is clearly visible on the electric component spectrogram. The plasmapause was crossed around 20.29 UT. Before that time, the constant frequency lines are waves generated by ground–based radio beacons or broadcast stations.

Fig. 2 (color plot): Dynamic spectrum of AKR observed during orbit 165. The frequency scale is compressed towards the high frequencies (see the text). The satellite was inside the plasmapause before 20.29:15 UT. Several AKR source crossings are observed between 20.32:30 UT and 20.33:45 UT when the lower cutoff of the emission crossed the f_{ce} (red) line. Note the broadband electrostatic activity at the edges of the source region and the fading of the VLF waves inside the AKR source.

These waves propagate in the whistler mode, which is cut at the local electron plasma frequency, whenever below f_{ce}. Since the cutoff of these lines is very sharp, we get a density profile of the plasmapause. As the satellite went out of it, an emission was recorded with an upper cutoff at the local upper hybrid frequency f_{uh} (about 280 kHz, at the left part of the figure) and a lower cutoff at the local f_{ce}; clearly, it is Z–mode radiation. The most intense part of the emission has a spin modulation phase shifted with respect to the one of the Z–mode emission. It consists of R–X – mode waves. The X–mode emission is reflected at the plasmapause. Further away, it has the characteristic bowl shape with an intensified lower edge which is either a propagation effect, or a caustic one (for a discussion of this event, see de Feraudy et al., 1987). A faint harmonic emission is observed above 400 kHz after 20.32:30 UT. The lower cutoff reached the electron gyrofrequency several times between 20.32:30 UT and 20.34:15 UT, corresponding to AKR source crossings as discussed below.

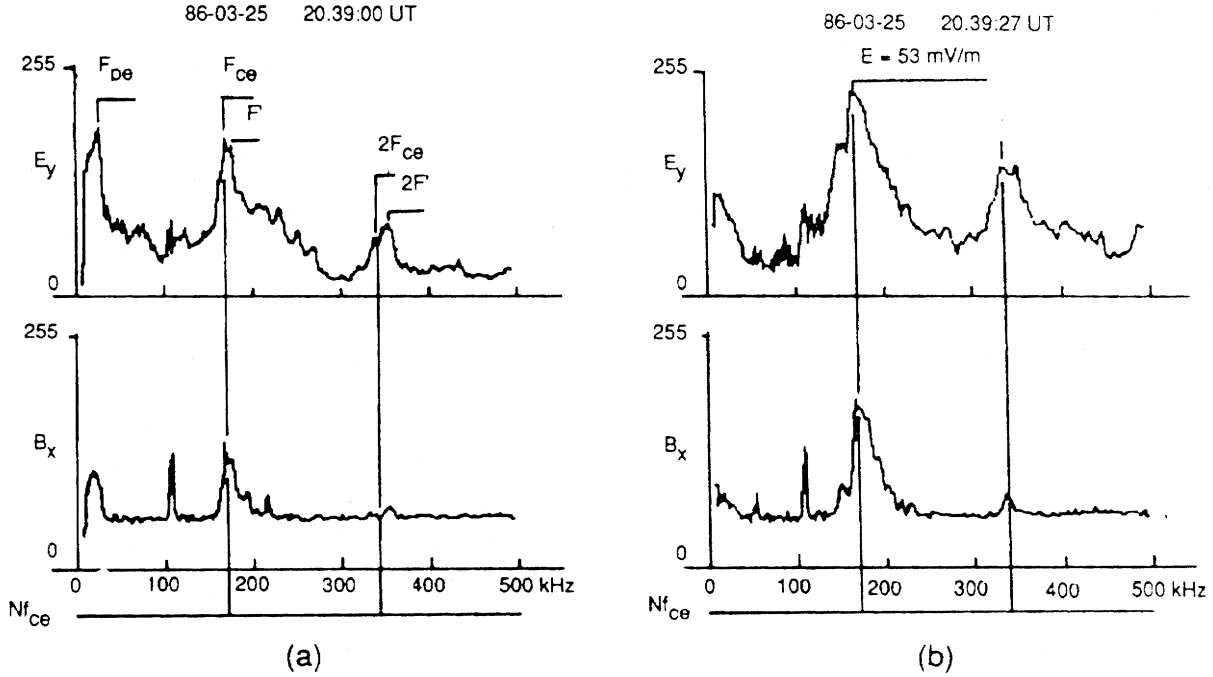

Fig. 3: Two sets of spectra were obtained during orbit 176, part (a) slightly before a source crossing, part (b) inside a source. The frequency axis is horizontal. The vertical axis represents the TM count–rate which is proportional to the spectral amplitude in dB. Vertical lines indicate the f_{ce} and $2f_{ce}$ locations. The upper spectra represent the wave electric components, the lower spectra the magnetic ones.

Individual SFA frequency scans of a strong AKR event (orbit 176) are presented in Figure 3. Spectrum (a) was observed slightly before crossing the source. Below the horizontal frequency scale, marks indicate the location of f_{ce} and $2f_{ce}$. Proceeding from the low frequencies towards the high frequency part of the spectrum, one meets successively a strong electrostatic emission with a sharp cutoff at the local plasma frequency, a region of electrostatic turbulence (Pottelette et al., 1987) and above f_{ce}, the main AKR emission with a harmonic component at $2f_{ce}$. Both the fundamental and the harmonic emissions

are electromagnetic. Since the amplifier of the magnetic sensor was far from saturation, one can conclude about the natural origin of the harmonic component, besides, considering the electric spectrum, one notices that the first two peaks of the fundamental emission have a harmonic counterpart with quite different relative amplitudes. The fine structure of the fundamental emission is clearly observed with five well defined peaks between f_{ce} and 280 kHz, to which two poorly resolved peaks must be added. Part (b) of Figure 3 will be analyzed in the next section.

3.2 AKR source crossings

Looking carefully at the lower edge of the electric component of the AKR emission in Figure 2, one sees that it crosses the f_{ce} line during three time periods, at 20.32:37 UT, between 20.33:00 UT and 20.33:30 UT, at 20.34:00 UT. This feature has been kept as a criterium to decide whether the satellite was inside a source or not. According to this definition an AKR source had been crossed three times, or three different sources had been encountered.

If such a criterium is accepted, then other observations organize quite well. Firstly, one remarks on the low frequency auroral hiss that during the source crossing the amplitude of the electric wave field fadded out. This can be interpreted as a drop of the cold plasma density which makes possible the VLF wave propagation. This was seemingly corroborated by the examination of the plasma density fluctuation (not shown here) derived from the electronic saturation current of the Langmuir probe operated by the low frequency wave V4L experiment, which showed a depression of the density curve at the time of the crossing of the source. On each side of the source region, strong broad band short duration electrostatic emissions were observed. They were identified as bursts of electrostatic noise (BEN). Such emissions were often, but not always, associated to source region crossings, conversely, they were sometimes observed without any generation of AKR. These bursts had occasionally amplitudes comparable to those of the AKR. The width of these source regions was, at most, between ten and one hundred kilometers.

The density gradients at the edges of the source regions had sometimes a noticeable effect on the wave characteristics. This is seen in Figure 4. This figure corresponds to orbit 176 where the two spectra of Figure 3 were observed. The upper four panels of the figure are the output of four high time resolution filterbank channels, with, from above, 512, 256, 128 kHz center frequency for AKR, 16 kHz center frequency for VLF waves. At the bottom, the V4L Langmuir probe current fluctuation measurements (labeled "δn/n" on the figure) are presented. The depression of the "δn/n" measurements is characteristic of a source crossing. A modulation at half the spin period is observed, it indicates that the observation of a vector quantity related to the magnetic field direction was superposed to the plasma fluctuations. It is presently not possible to state whether it was a static electric field signature or simply the result of a drift motion of the electrons. A noticeable shift in the phase of the spin modulation of the AKR emission is clearly seen at 20.39:20 UT when the satellite entered the source. It indicates a rotation of the polarization plane which resulted from a rotation of the wave normal. It might be caused by a mode conversion on

the density gradient, or, more likely, by a refraction of the waves at the edge of the density structure corresponding to source region. This strong refraction is necessarily associated with a partial reflexion at the density gradient, which is a primary condition for a lasing effect to take place. Such an important rotation of the polarization plane was not usually observed.

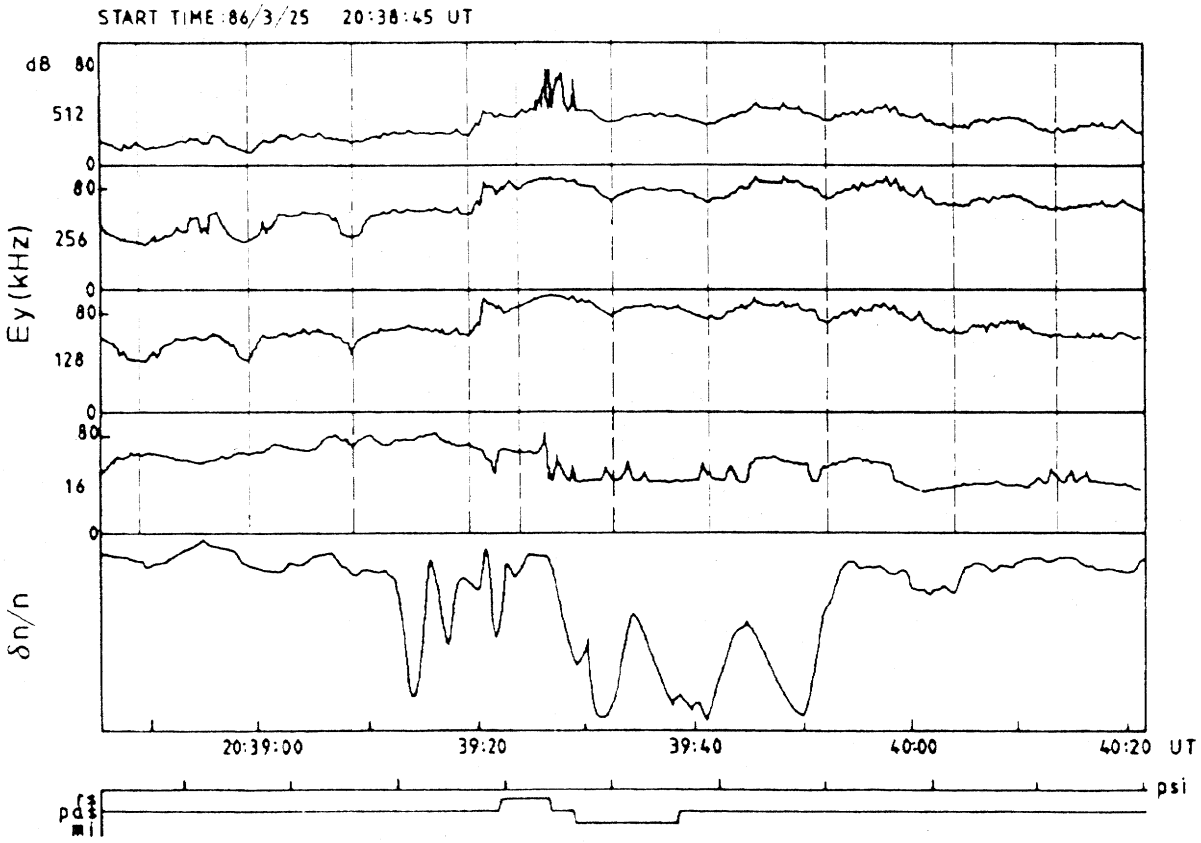

Fig. 4: Filterbank and Langmuir probe electron current ("δn/n") outputs as a function of time. The three upper panels correspond to filters with a center frequency inside the AKR frequency range. The fourth channel is in the VLF range. The center frequency of the filters is indicated on the left of the panels. The lower panel is the output of the "δn/n" V4L experiment. It gives an indication on the density and/or average electron energy fluctuations. Note the density depression, strongly spin modulated, inside the source of AKR. Below the time scale, tickmarks on the "psi" line, above the status line of the experiment, indicate the time when the antennae were closest to the field aligned direction.

A wave spectrum obtained as the satellite was inside the source is presented in Figure 3(b). One notices a secondary peak below f_{ce}. It is not present on the spectrum of Figure 3(a) which was obtained at 20.39:00 UT, just before entering the source region therefore it consists probably of a wave trapped inside the source region. The amplitude of the main peak reaches 53 mV/m.

3.3 AKR sources and auroral discrete arcs

Viking observations showed unambiguously that AKR source regions are magnetically connected to auroral discrete arcs, whether these arcs are located on the auroral oval or at much higher latitudes.

The upper panel of Figure 5 presents a set of 6 consecutive V5 UV imager pictures obtained during orbit 849. The satellite was over the northern polar cap. The white circle indicates the 65° magnetic latitude line at the ionospheric level. The white line indicates the magnetic midnight. Time (UT) is indicated on the right, below each frame. The footprint of the magnetic field–line passing through Viking is marked by a white spot. In these pictures it is seen that an auroral surge developed on the post midnight side of the oval. It was reached by the footprint of the Viking field–line at about 06.29 UT. The AKR observations along the same orbit are presented on the middle panel. All the characteristic features of the source crossings that were stated above are observed from 06.28:00 UT to 06.29:15 UT which is the time when the Viking field–line crossed the auroral surge. A clear signature is also observed on the particle data presented in the bottom panel fluxes. A characteristic change in the pitch angle distribution of the electrons is seen at the time of the source crossing. Then most of the particle with energy below 3 keV were removed whatever the pitch angle, leading to a kind of broad ring distribution with a loss cone of the energetic electrons. On the ion data a characteristic upflowing beam was observed.

Another example of the simultaneous crossing of an auroral arc and of an AKR source region is shown in Figure 6 corresponding to orbit 1315. Here the arc crossing occurred at quite a different place, at a higher latitude, on the morning MLT sector. The time of the arc crossing was about 22.56 UT as is seen on the upper panel. The lower panel presents the corresponding wave data. The source crossing was well defined around 22.56 UT. The small discrepancy in local time could originate in the choice of the geomagnetic field model used for the field line mapping into the ionosphere.

Fig. 5 (color plot): Composite figure of UV aurora images (top panel), high frequency wave (middle panel) and particle (lower panel) observations during orbit 849. The simultaneity of the arc crossing by the Viking field–line footprint and the AKR source crossing appears clearly. At the same time, a significant change in the distribution of the electron velocities is observed, an intense beam of upflowing ions is observed simultaneously.

Fig. 6 (color plot): Observations as those of Figure 5, for orbit 1315. The UV imager pictures and the wave observations are only presented.

3.4 Dayside observations of AKR

Observations of AKR on the dayside were less frequent than on the nightside. About ten cases have been examined up to now from the available processed data. They were characterized by the following features:

- The invariant latitude range of the observations was typically 3°, this width is much smaller than the one of nightside AKR observations.
- Dayside AKR was mostly observed equatorward of the edge of the oval.
- The morphology of the emissions was similar to the dayside observations presented in Figure 1 for orbit 185, namely recurrent bursts of about one minute duration with a period of few minutes.
- The dayside observations were generally well separated from the "nightside" ones.

Up to now we have not found evidence for AKR source crossings on the dayside. The reason is probably to be found in the fact that Viking always passed through the dayside of the auroral oval close to the apogee. The similarity of the orbit characteristics (altitude and Magnetic Local Time) over the dayside oval could be the origin of the similarity of the corresponding AKR observations.

4. Conclusions

The Viking observations of AKR confirmed that this emission is generated at f_{ce}. The high frequency resolution of the V4H Swept Frequency Analyzer hinted that the waves could even be created below the electron gyrofrequency. If no cold plasma is present the relativistic dispersion relation of the R–X mode allows a cutoff frequency f_x below f_{ce}, thus a generation of the R–X mode AKR is possible very close to, or below the electron gyrofrequency. However, the relative frequency separation of f_x from f_{ce} is of the order of magnitude of a^2/c^2 where a is the r.m.s. velocity of the electrons and c is the light velocity. For 1 keV electrons, when $f_{ce} = 200$ kHz, a typical value for AKR observed by Viking, the frequency separation f_x–f_{ce} is of the order of 1 kHz which is smaller than the frequency resolution of the instrument in this frequency range. The only way for this experiment to provide direct evidence for this relativistic effect is either to meet AKR sources at altitudes such that $f_{ce} < 128$ kHz, since in this frequency range, the resolution of the instrument is only 1 kHz, or to find sources with higher energy particles (i.e. above 2.5 keV when $f_{ce} = 200$ kHz).

The altitude range of Viking was well suited for frequent crossings of particle acceleration regions with AKR sources. Combined with this particularity, the high time resolution of the V4H instrument made possible a detailed observation of these sources. Besides, the presence of an imager on board allowed a direct correlation between the location of the source regions of AKR and magnetically conjugate auroral arcs.

A first analysis indicated that the AKR source regions are narrow structures with a width ranging from a few kilometers to several tens of kilometers, depending partly on the angle between the spacecraft trajectory and the direction of the arcs. The source structures are presumably field aligned yet, this deserves a careful examination.

It was shown that the source regions of AKR have a very low density of cold electrons with respect to the surrounding plasma. However, a substantial amount of hot particles is present, a quantitative assessment of this remains to be done. The average energy of the particles responsible for the AKR generation is not necessarily higher than the energy of the particles outside the source, nevertheless the distribution of their velocities in velocity space is quite different. Several cases of ringlike distribution functions with a cold core were observed, in all the cases a loss cone was present.

Significant refractive effects at the edges of AKR source structures were observed during a strong AKR event, this is in favour of a feedback mechanism with lasing effects similar to the model proposed by Calvert (1982).

It was shown that AKR source structures are a part of fieldlines connected to auroral arcs. On the examples presented here, no particular bright spot or other localized structure was observed at the connection point, suggesting the possibility for AKR source structures elongated in the direction the arcs. It was shown that the source structures can be encountered in quite different regions of the auroral and polar area.

Often associated with the AKR source regions, intense bursts of broadband electrostatic noise are observed at the edges of the plasma structures.

Several times AKR was observed over the dayside. There, the emissions consisted of bursts with about one minute duration. Dayside AKR was encountered at the equatorward edge of the auroral oval. Presently it is impossible to decide whether these waves were generated on the dayside or they were propagating from a distant source located on the nightside of the high latitude regions.

Acknowledgements: The Viking project was managed and operated by the Swedish Board for Space Activities. The authors are grateful to the V3, V4L and V5 experimenters who kindly provided them with particle data, plasma probe current data and UV images. R. Pottelette is also thanked for valuable discussions and J. Paris for the production of some of the V4H color prints.